Research Article

C. Anil Kumar Reddy*, Pothamsetty Kasi V. Rao, Begori Venkatesh and Boggarapu Nageswara Rao

Influence of liquid nitriding on the surface layer of M50 NiL steel for bearing applications

https://doi.org/10.1515/jmbm-2025-0050 received December 28, 2024; accepted February 27, 2025

Abstract: The synergistic effects of liquid nitriding (LN) duration and temperature on the characteristics of the nitriding region formed on M50NiL steel have been systematically examined. The nitriding procedure is conducted at temperatures 525, 550, 560, and 570°C for durations 3, 6, 8, and 12 h. This nitriding methodology enhances not only the hardness but also other attributes such as wear resistance, fatigue resistance, and surface hardness. The resulting nitrided layers are characterized through optical microscopy, scanning electron microscopy coupled with energy-dispersive X-ray spectroscopy (EDS), and X-ray diffraction analysis. The findings indicate that the thickness of the nitride layer increases in correlation with the nitriding temperature. Empirical data demonstrated that the nitrides ε-Fe₂₋₃(N, C) and γ'-Fe₄(N,C) present within the compound layer contribute to the enhancement of microhardness. The study emphasizes the effect of LN duration on the tribological and chemical properties of the specimen. When M50NiL bearing steel is subjected to liquid nitriding at 525°C, the resulting nitrided layer primarily consists of a thin ε-Fe₂₋₃N layer. The depth of the nitrided layer exhibited significant variation with increasing treatment temperature. The liquid nitriding process effectively enhanced the surface hardness. Energy-dispersive X-ray spectroscopy (EDS) analysis indicated an increased concentration of nitrogen in the nitrided sample treated at 560°C for 12 h. The steel specimen identified as LN525, which was nitride for 8 h, exhibited superior wear resistance compared to the other nitrided samples. Polarization studies reveal that after a 12 h nitriding period at 570°C, the developed expanded austenite began to contract concurrently with a reduction in the thickness, hardness, and corrosion resistance of the nitrided layer. The effects

Begori Venkatesh: Mechanical Engineering, Vardhaman College of Engineering, Hyderabad, 501218, India

of prolonged nitriding time were attributed to the diminished chemical potential of nitrogen within the salt bath, resulting in the outward diffusion of nitrogen from the sample to the salt bath. Following nitriding at 525°C for 8 h, the nitrided layer of M50NiL steel demonstrated exceptional corrosion resistance.

Keywords: liquid nitriding, corrosion resistance, microhardness, compound layer, X-ray diffraction

1 Introduction

Liquid nitriding (LN) is a widely recognized diffusion methodology, which is, in fact, liquid nitrocarburizing, a thermochemical reaction through which nitrogen, predominantly, and a minor quantity of carbon are infiltrated into the surface of ferrous materials. The nitrogen interacts with the iron to generate a layer of iron-nitride compound, which enhances surface characteristics, such as augmenting resistance to wear, friction, corrosion, and fatigue [1]. The process of LN can be conducted at temperatures ranging from a minimum of 500°C to a maximum of 630°C. Typically, however, the operational temperature range is situated between 540 and 590°C. All surface treatment methodologies inevitably result in some degree of dimensional alteration of the components, yet LN results in comparatively minimal growth, typically measuring 0.0002-0.0003 in (5–8 µm) in diameter. The compositions of case-producing salts may differ among manufacturers, but they primarily consist of sodium and potassium cyanides or sodium and potassium cyanates. The cyanide, which acts as the active component, undergoes oxidation to cyanate through the aging process, as detailed below. The commercial salt amalgamation (60-70% sodium salts and 30-40% potassium salts) is subjected to melting at temperatures ranging from 540 to 595°C [2]. During the melting phase, a protective cover should be utilized over the retort to prevent spattering or potential explosion of the salt unless the apparatus is entirely hooded and adequately vented.

During the process of LN, the substrates are submerged in a molten salt bath for a specified duration, which typically spans several hours. Nitrogen permeates the surface of the

^{*} Corresponding author: C. Anil Kumar Reddy, Department of Mechanical Engineering, Koneru Lakshmaiah Education Foundation, Vaddeswaram, 522502, India, e-mail: anilreddymechanical@gmail.com Pothamsetty Kasi V. Rao, Boggarapu Nageswara Rao: Department of Mechanical Engineering, Koneru Lakshmaiah Education Foundation, Vaddeswaram, 522502, India

2 — C. Anil Kumar Reddy et al. DE GRUYTER

substrate, leading to the formation of a compound layer that significantly enhances the material's characteristics. This compound layer is composed of nitrides, carbides, and carbonitrides, which are contingent on the composition of the salt bath and the particular process parameters employed. Upon the completion of the designated treatment duration, the substrates are extracted from the salt bath and subsequently undergo a cooling phase to ensure the stabilization of the compound layer. The rate of cooling is meticulously regulated to avert any distortion or fracturing of the substrate. Following the cooling process, the substrates are generally subjected to a rinsing procedure to eliminate any residual salt and are then evaluated for quality before proceeding to further processing or utilization in various applications.

A major benefit of LN lies in its capacity to generate a uniform and meticulously controlled compound layer over the entire surface of the substrate. This layer markedly enhances wear resistance, hardness, and corrosion resistance while preserving the intrinsic properties of the substrate material. Furthermore, LN is applicable to a diverse array of ferrous and non-ferrous metals, encompassing carbon steels, alloy steels, stainless steels, and even select non-ferrous substances [3].

In comparison to the current surface hardening techniques like carburizing, the goal of this study is to inexpensively and effectively improve the surface properties of high-temperature bearing steels, such as M50 NiL steel. The results indicate a notable improvement in surface qualities.

1.1 Influence of LN on bearing steels

LN markedly improves the operational characteristics of bearing steels through the enhancement of their surface attributes. This methodology entails the diffusion of nitrogen into the superficial layer, leading to an increase in wear resistance and fatigue strength, both of which are imperative for the durability of bearings when subjected to operational stress. Furthermore, nitrogen alloying is crucial in increasing the strength and hardness of low-carbon austenitic steels, rendering them exceptionally appropriate for bearing applications. The development of an S-phase layer during the nitriding process contributes to these enhancements by generating expanded austenite, which not only improves mechanical properties but also enhances corrosion resistance. This phenomenon is particularly advantageous for austenitic stainless steels, which are frequently utilized in the manufacture of bearings due

to their remarkable corrosion resistance and mechanical properties [4]. In summary, LN, as a surface treatment technique, adeptly amalgamates these advantages, ensuring that bearing steels are capable of enduring severe conditions while preserving performance and durability [5]. Consequently, the incorporation of LN in the treatment of bearing steels represents a strategic initiative to augment their operational efficacy and lifespan.

Nitriding can be executed using four distinct mediums: (1) liquid, (2) gas, (3) plasma, and (4) fluidized bed. All methodologies aim to achieve comparable - albeit not identical – outcomes. Nevertheless, LN is regarded as the standard for uniformity, consistency, and versatility. LN also offers the most effective combination of wear and corrosion resistance alongside the shortest processing durations. It constitutes a diffusion process that alters the surface characteristics of the treated component. This modified surface layer is seamlessly integrated with the bulk material, thereby rendering it impervious to flaking or peeling. Authentic heat treatment processes function at elevated temperatures and modify the crystal structure of the steel to yield the desired mechanical properties. LN attains its results through a chemical reaction (at temperatures lower than those employed in conventional heat treatment) that facilitates the formation of a hard nitride compound upon the surface of the component [6].

LN constitutes a sophisticated surface-hardening technique that markedly elevates the mechanical and corrosive characteristics of steel, with particular emphasis on 316 stainless steel. The following delineates the principal advantages obtained from this methodology:

- (a) Increased hardness: LN engenders a considerable augmentation in surface hardness. For example, the Vickers hardness of 316 stainless steel can increase from 220 to 818 HV subsequent to a nitriding duration of 4 h at a temperature of 425°C. This enhancement is ascribed to the diffusion of nitrogen into the steel matrix, which induces lattice distortion, thereby fortifying hardness through mechanisms of solid solution strengthening [7,8].
- (b) Formation of expanded austenite: The nitriding procedure facilitates the development of a singular expanded austenite phase at the material's surface. This phase is of paramount importance as it plays a significant role in augmenting both the hardness and corrosion resistance of the steel substrate. However, extended nitriding durations may precipitate denitriding phenomena, which could compromise the thickness and intrinsic properties of the nitriding layer.
- (c) Enhanced corrosion resistance: Nitrided specimens demonstrate markedly superior resistance to localized corrosion in comparison to their untreated steel

counterparts. The incorporation of nitrogen within the passive layer serves to repel aggressive anionic species such as chloride, which are notorious for instigating pitting corrosion. Consequently, this phenomenon results in an expanded passive range and a minimized hysteresis loop during cyclic polarization assessments, thereby indicative of enhanced corrosion resilience [9].

- (d) Optimized nitriding conditions: The investigative study elucidated optimal nitriding parameters, such as a nitriding duration of 4 h at 475°C, which culminated in a more favorable amalgamation of hardness and corrosion resistance. The significance of this optimization lies in its capacity to harmonize the advantages of increased nitrogen solubility with the potential hazards associated with denitriding [10].
- (e) Depth of hardness improvement: The enhancement in hardness is observed to extend to a depth of approximately 100 µm beneath the surface, thereby indicating that the advantages of nitriding transcend mere surface alterations. This depth of hardness improvement is attributable to the effective diffusion of nitrogen into the steel substrate.

LN substantially ameliorates the mechanical and corrosive properties of steel through the augmentation of hardness, the formation of advantageous microstructural features, and the optimization of treatment conditions to attain optimal performance outcomes [11].

2 Experimental procedure

2.1 Material

The experimental M50NiL alloy is fabricated utilizing a vacuum induction melting and casting apparatus, succeeded by processes of forging and thermal treatment. The elemental composition of M50NiL alloy is shown in Table 1. Specimens of M50NiL alloy with dimensions measuring 10 mm × 10 mm × 5 mm are employed in the current investigation. M50NiL alloy represents a specialized iteration of M50 steel, engineered to augment the functionality of thrust bearings [12]. This alloy demonstrates a markedly enhanced fatigue life, reportedly prolonging its operational duration by a factor of six in comparison to conventional M50 steel; the superior performance of M50NiL is ascribed to the existence of residual compressive stresses within its subsurface regions, which bolster its durability and resistance to spalling fatigue [13]. The attributes of M50NiL alloy

Table 1: Chemical composition of M50NiL steel (wt%)

С	Cr	Мо	Ni	٧	Mn	Si	Fe
0.12	4.1	4.0	3.2	1.1	0.1	0.1	Balance

are further refined through targeted thermal treatment methodologies, such as NiL treatment, which enhance its fatigue life and wear resistance. This treatment is pivotal for preserving the elevated surface hardness characteristic of M50 alloys, which typically exceeds 60 HRC and falls within the range of 65-72 HRC, a crucial requirement for applications in roller bearings [14].

2.2 LN

The LN process serves to augment the hardness, wear resistance, and corrosion resistance of metallic surfaces. In this particular methodology, CR4 powder or CR2 tablets, in conjunction with 5 g of sulfate, represent the fundamental composition, which is critical in influencing the properties of the treated material. Generally, the composition consists of 65% sodium salts and 35% potassium salts, although a ratio of 75:25 may also be utilized in specific instances. This meticulous selection of salts is deliberately made to attain the anticipated nitriding effects, thereby ensuring optimal functionality of the treated components [15].

Before initiating the nitriding process, it is imperative to adequately prepare the samples to ensure effective treatment. This preparation entails a comprehensive cleaning of the samples to eradicate any contaminants or surface impurities that may impede the nitriding process. The samples undergo a cleaning procedure in an ultrasonic water bath, employing high-frequency sound waves to dislodge dirt and debris from the surface, thereby establishing pristine conditions for the nitriding treatment. Subsequent to the cleaning procedure, the samples are primed for the nitriding treatment [16]. In this particular nitriding experiment, the samples are subjected to treatments at temperatures of 525, 550, 560, and 570°C for durations of 3, 6, 8, and 12 h comprising 12 samples. Throughout the treatment process, the samples are immersed in the nitriding composition at the designated temperature and duration, as illustrated in Figure 1(a) and (b). This procedure facilitates the controlled diffusion of nitrogen atoms into the surface of the samples, culminating in the formation of a hardened layer that significantly enhances their mechanical properties. Upon the conclusion of the treatment, the



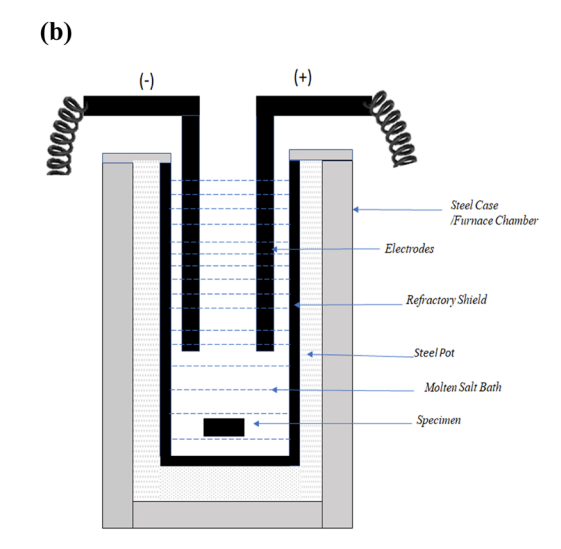


Figure 1: (a) LN furnace, and (b) LN furnace 2D Diagram.

samples are systematically cooled to ambient temperature to avert distortion or cracking, thus ensuring the integrity of the treated components.

3 Results and discussion

3.1 Phase structure and microstructure

Utilizing the X-ray diffraction (Bruker AXS, D8 Advance X-ray Diffraction system) with Cu-K α radiation (λ = 0.15406 nm) in the range of angles 20°–120° at 40 kV and 30 mA with 0.02° interval step mode, the phase structure of the nitrided surface is examined.

Figure 2(a) illustrates the X-ray diffraction patterns for LN at 525°C, where a substantial presence of α-FeN is detected. As the duration of treatment is extended, the diffraction intensity corresponding to y-FeN and Fe₃O₄ exhibited an increase, while the intensity associated with α-FeN diminished. Examination of the diffraction patterns reveals significant disparities in the peak intensities of γ-FeN and the iron oxide (Fe₃O₄), underscoring the gradual evolution of these phases over time. The presence of α -Fe is markedly diminished following an 8 h nitriding process as the nitride layers assert their dominance. This transformation correlates with the enhanced wear and corrosion resistance of the sample, as the formation of robust nitride phases augments the surface characteristics of the material. As the duration of nitriding extends, a general decrease in the intensity of the γ-Fe₃N peaks is observed. Nevertheless, after a nitriding period of 12 h, a distinct increase in the γ-Fe₃N peak intensity is observed. The slight

broadening of the peaks may suggest the presence of stress or strain within the layer resulting from extended nitriding. With prolonged nitriding periods, the diffusivities of nitrogen and oxygen within the nitriding medium increase. Consequently, a greater quantity of nitrides and oxides, such as γ -FeN and Fe₃O₄, is produced, leading to an increased depth of the nitrided layer.

At a reduced treatment time of 550°C, a larger quantity of α-FeN is observed, as shown in Figure 2(b). As the treatment duration increased, the diffraction intensity of α-FeN experienced a decline. This reduction can be attributed to the gradual formation and proliferation of alternative nitride phases, such as γ-FeN and Fe₃O₄, which gain prominence over time. The intensity of the γ-Fe₃N phase intensifies after 6 h of nitriding. This enhancement in intensity is a result of the ongoing diffusion of nitrogen into the steel substrate, facilitating the growth of γ-Fe₃N. As the nitriding process advances, the formation of y-Fe₃N becomes more extensive, thereby contributing to the increased hardness and wear resistance of the material. The nearly complete absence of Fe₃O₄ peaks corroborates that the oxide layer has been entirely transformed into nitrides. A review of the diffraction patterns reveals notable differences in the peak intensities of y-FeN and the iron oxide (Fe₃O₄), emphasizing the progressive development of these phases over time.

The X-ray diffraction (XRD) patterns elucidate the existence of γ -FeN, γ -Fe $_3$ N, and α -Fe phases, alongside a minor detection of Fe $_3$ O $_4$ in the specimens subjected to LN560 treatment, as shown in Figure 2(c). The γ -FeN phase emerges as the most prevalent phase across all examined samples, corroborating the hypothesis of a nitride layer formation ensuing from the LN process. The γ -Fe $_3$ N phase

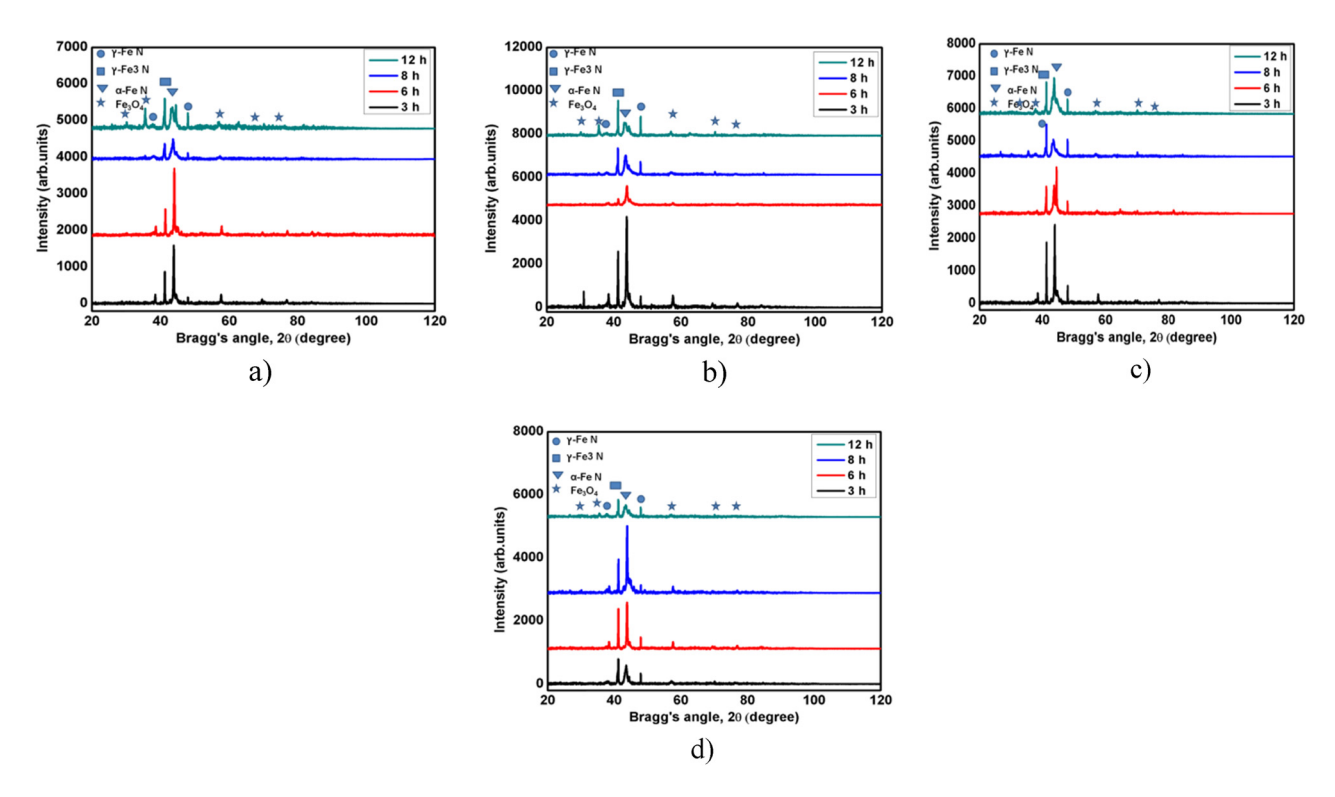


Figure 2: (a)-(d) XRD profiles for LN samples (525-570°C). XRD plot (a) for LN525°C, (b) for LN550°C, (c) for LN560°C, and (d) for LN570°C.

also prominently contributes to the overall hardness and wear resistance of the samples. The intensity of the α -Fe peak, which indicates the ferrite phase, exhibits a progressive decrease in intensity as the nitriding duration is extended, suggesting that nitrogen diffusion is increasingly efficient with lengthier nitriding periods. At a treatment temperature of 560°C, the y-FeN peaks exhibit intensification up to a nitriding duration of 8 h, indicating the gradual establishment of this nitride phase. However, beyond the 8 h mark, a noticeable decline in the y-FeN phase is observed. This phenomenon can be ascribed to the transformation of y-FeN into more stable and potentially coarser phases or compounds as the nitriding process advances. The extended exposure to elevated temperatures may facilitate the decomposition of y-FeN or its conversion into phases such as α-FeN, leading to a diminished representation of y-FeN in the XRD patterns post 8 h. The decreased representation of Fe₃O₄ at extended nitriding duration indicates the development of a more protective nitride layer endowed with superior corrosion resistance properties. The compact and densely packed nitride phases serve as a protective barrier, thereby mitigating the diffusion of corrosive agents.

At an elevated nitriding temperature of 570°C, a negligible quantity of α -FeN is observed in Figure 2(d). With the extension of the nitriding treatment duration at 570°C, the

diffraction intensity corresponding to α-FeN and y-Fe₃N phases exhibited an enhancement, reaching a peak at 8 h. However, the intensity of γ-Fe₃N experienced a substantial reduction following 8 h of treatment, indicative of a decrease in its prevalence. Moreover, the presence of α -FeN markedly diminishes after 8 h, coinciding with the establishment of dominant nitride layers. This alteration in phase composition is associated with the enhanced wear and corrosion resistance observed in the samples, as the emergence of robust nitride phases such as y-FeN augments the surface properties, rendering the material more resilient to mechanical and chemical degradation. The diffraction patterns reveal conspicuous discrepancies in the peak intensities of y-FeN and iron oxide (Fe₃O₄), underscoring the progressive formation of these phases over time. Generally, the intensity of the y-FeN peaks increases concomitantly with the increase in the treatment duration. The slight broadening of the peaks may suggest the presence of stress or strain within the layer due to prolonged nitriding. Nonetheless, the resurgence and augmented intensity of Fe₃O₄ after 12 h imply that extended nitriding may result in surface oxidation, potentially compromising the material's corrosion resistance. At 12 h, distinct and discernible peaks of α-FeN, y-Fe₃N, y-FeN, and Fe₃O₄ are observable when compared to the 8 h mark. However, the peaks displayed are broadened, which may

be attributed to the intensified formation of these phases and the concomitant residual stresses within the nitrided layer. The extended nitriding duration can induce more pronounced structural modifications and phase transitions, which contribute to the peak broadening observed in the XRD patterns.

Nitrogen diffusivity can increase with increasing nitriding temperature, which can reduce the amount of nitrogen present at the surface. The phase type of the compound layer is unaffected by the nitriding temperature. The peak intensity of the iron nitrides in the compound layer is altered by variations in the temperature and duration of nitriding. Large-size iron nitrides are more likely to form in the compound layer during nitriding at high temperatures, as evidenced by the fact that the peak intensity is maximum at 560°C.

3.2 EDS analysis of LN samples

EDS is performed utilizing a Nova 450 system integrated with a scanning electron microscope (SEM, thereby facilitating a comprehensive analysis of the chemical composition of the specimen. The nitrided M50NiL samples are subjected to EDS analysis to ascertain their chemical composition, with

a particular emphasis on the nitrogen content. EDS measurements are conducted at two randomly selected locations on the nitrided surface. Figure 4 presents the EDS findings for the LN layer of the M50NiL specimens, acquired after varying durations (3, 6, 8, and 12 h) of nitriding at temperatures of 525, 550, 560, and 570°C.

As shown in Table 2 and Figure 3(a), the weight percentages of components identified in the EDS spectroscopy analysis for the untreated M50NiL specimen are as follows: 9.9% carbon (C), 0.1% aluminum (Al), 0.2% silicon (Si), 0.1% titanium (Ti), 1.1% vanadium (V), 3.6% chromium (Cr), 0.3% manganese (Mn), 76.4% iron (Fe), 0.9% cobalt (Co), 2.8% nickel (Ni), 0.1% copper (Cu), 4.2% molybdenum (Mo), and 0.4% tungsten (W).

The EDS analysis conducted at 525°C indicated that the LN525°C sample at 6 h exhibited an increased surface nitrogen content (4.0 wt%), whereas the LN520°C sample at 8 h demonstrated a diminished nitrogen concentration (0.4 wt%), as shown in Figure 3(b). The increased nitrogen content observed in the LN525°C sample at 6 h indicates a more proficient nitrogen diffusion into the surface layer, which is imperative for the enhancement of surface hardness and wear resistance. This augmented nitrogen content can be attributed to the optimal nitriding conditions, wherein the temperature and duration promote the

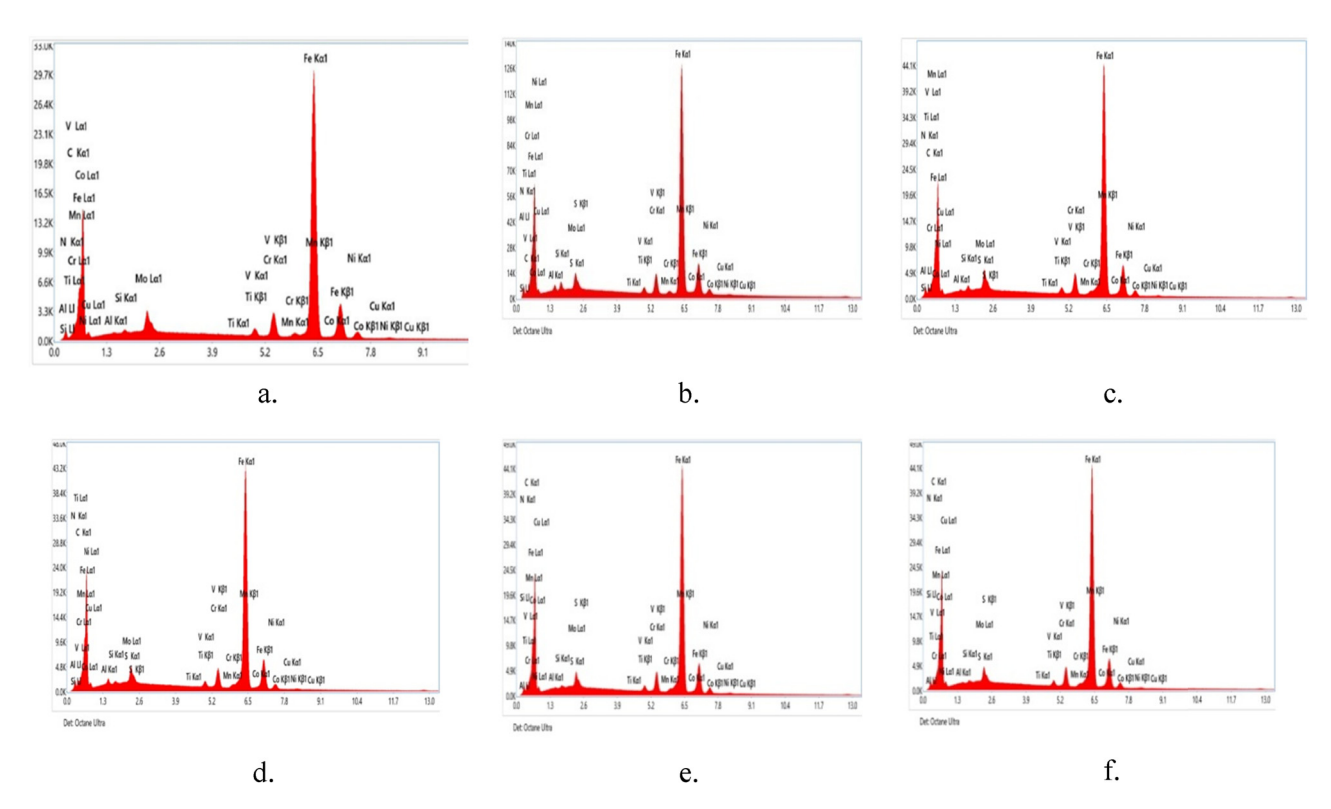


Figure 3: (a)–(f) EDS analysis of LN M50NiL specimens at 525 for 3,6,8 and 12 h: (a) untreated sample, (b) LN525°C at 6 h, (c) LN550°C at 6 h, (d) LN560°C at 12 h, (e) LN570°C at 12 h, and (f) LN550°C at 12 h.

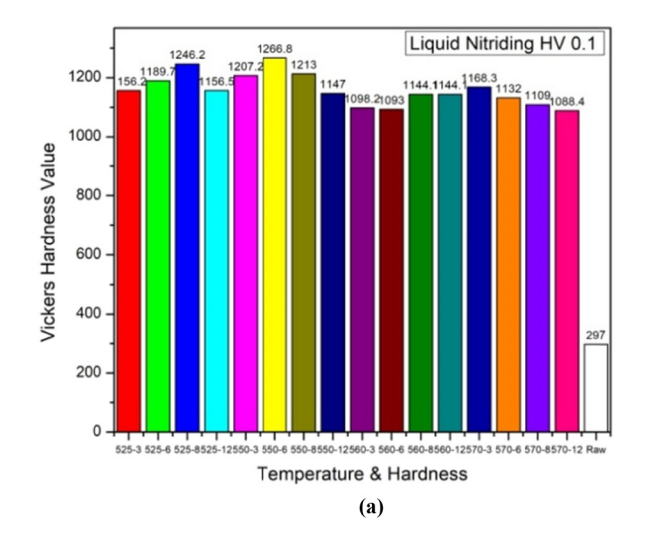
Table 2: EDS analys	s of LN M50NiL	specimens at 525-570	°C for 3, 6, 8, and 12 h
---------------------	----------------	----------------------	--------------------------

Element (wt%)	Untreated	LN525@06	LN550@06	LN560@12	LN570@12	LN550@12
Carbon (C)	9.9	14.6	11.2	11.7	9.6	3.0
Nitrogen (N)	0.0	4.0	6.7	8.2	7.5	0.0
Aluminum (Al)	0.1	0.6	0.1	0.7	0.2	0.0
Silicon (Si)	0.2	0.7	0.4	0.2	0.2	0.6
Sulfur (S)	0.0	0.4	0.0	0.0	0.0	1.2
Titanium (Ti)	0.1	0.0	0.1	0.1	0.1	0.0
Vanadium (V)	1.1	0.7	1.0	1.0	1.0	0.6
Chromium (Cr)	3.6	2.9	3.3	3.1	3.3	3.2
Manganese (Mn)	0.3	0.1	0.4	0.3	0.3	0.0
Iron (Fe)	76.4	67.7	69.1	67.5	70.9	84.7
Cobalt (Co)	0.9	2.2	1.3	1.3	1.1	2.0
Nickel (Ni)	2.8	3.1	2.6	2.4	2.6	3.6
Copper (Cu)	0.1	0.6	0.1	0.2	0.1	0.5
Molybdenum (Mo)	4.2	2.5	3.8	3.2	3.2	0.5

establishment of a stable nitride layer. A negligible quantity of sulfur (0.4 wt%) is detected in the LN525°C sample at 6 h, with its influence on material properties anticipated to be minimal due to the relatively low concentration. Furthermore, the carbon content increases to 14.6 wt% in comparison to the untreated sample, thereby contributing to improved mechanical properties.

At 550°C, nitrogen is absent in the LN550°C sample at 12 h, indicating that nitrogen did not effectively diffuse into the material to establish a nitrided layer, likely attributable to factors such as insufficient temperature, inadequate time, or the composition of the material. Moreover, a sulfur content of 1.2 wt% following 12 h in the nitriding process suggests extended exposure, likely resulting in considerable modifications to the material's properties.

Figure 3(c) reveals a nitrogen concentration of merely 1.2 wt% in the LN560 sample at 6 h, which is markedly lower than that observed in the other samples subjected to nitriding at 560°C. This comparatively diminished nitrogen concentration implies that the nitriding procedure during this particular duration (6 h) may have been inadequate for facilitating optimal nitrogen diffusion into the surface layer, subsequently resulting in a less pronounced hardening effect. The LN560°C sample at 12 h displays a nitrogen content of 8.2 wt%, indicative of a higher surface nitrogen concentration, and concurrently exhibits a carbon content of 11.7 wt% as shown in Figure 3(d). This observation elucidates a more efficient and extended nitrogen diffusion process, culminating in an increased surface nitrogen concentration. The protracted nitriding duration facilitates a more



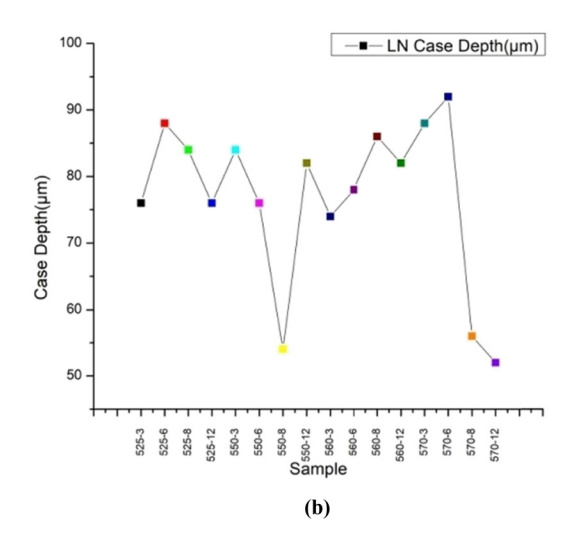


Figure 4: (a) Hardness profiles of the LN specimens, and (b) case depth profile of LN specimens.

8 — C. Anil Kumar Reddy et al. DE GRUYTER

significant formation of nitrides, thereby augmenting surface hardness and resistance to wear.

For the LN570°C specimen at 12 h, which underwent a more extensive nitriding duration of 12 h, there is a notable increase in nitrogen content (7.5 wt%) alongside a carbon content of 9.6 wt%, as shown in Figure 3(e). Conversely, the 3-h nitrided sample (LN570°C at 3 h) reveals a diminished nitrogen content of 0.1 wt%, in conjunction with a carbon content of 3.5 wt% and an iron content of 81.1 wt%, which is intriguingly higher than that of the untreated sample (76.4 wt%). Additionally, the formation of 12.7 wt% of terbium (Tb) in the LN570°C at 6 h sample indicates the integration of this element into the material's microstructure, potentially enhancing mechanical attributes such as toughness and fatigue resistance. Furthermore, terbium may contribute to improved corrosion resistance through the formation of protective compounds.

The outcomes from the EDS analysis unequivocally demonstrate that the nitrogen content within the steel increases with the duration of the nitriding solution, notwithstanding that the EDS measurements are obtained from randomly selected points across the steel surface. Nitrogen is absent in the LN550°C sample at 12 h, while the peak nitrogen content of 8.2 wt% is recorded in the LN560°C sample at 12 h, as shown in Figure 3(f). This extensive variation underscores the influence of nitriding parameters, particularly temperature and duration, on the incorporation of nitrogen into the steel matrix. The LN550°C sample at 12 h, characterized by undetectable nitrogen levels, suggests inadequate nitriding under the specified conditions, whereas the LN560°C at 12 h sample, exhibiting the maximum nitrogen content, reflects optimal conditions for nitrogen uptake, thereby enhancing surface characteristics. An elevated nitrogen concentration correlates with improved wear resistance and surface durability. This finding indicates that, in general, at lower temperatures, a reduced nitriding duration permits greater diffusion of nitrogen into the steel matrix. In contrast, at elevated temperatures, moderate or extended nitriding durations prove sufficient for effective nitrogen uptake.

3.3 Surface mechanical properties (hardness, corrosion, and wear)

3.3.1 Microhardness

The microhardness profiles of the nitrided layers are assessed utilizing a Vickers microhardness tester (ECONO-MET VH 1MD) under a load of 100 g for a duration of 20 s. In

order to ensure measurement accuracy, the mean value derived from three indentations made at identical depths within the nitrided layer is employed. The microhardness profile of the nitrided samples, subjected to nitriding temperatures and soaking durations ranging from 525 to 570°C and from 3 to 12 h, respectively, is illustrated in Figure 4(a). The surface microhardness of the nitrided M50NiL steel exceeds 1,000 HV, indicating that LN can substantially enhance surface microhardness. The hardness of the unprocessed M50NiL specimen is approximately 297 HV. The cyanate concentration within the bath is pivotal in determining the extent of nitrogen diffusion through the surface. Consequently, an elevated cyanate concentration in the bath results in a thicker nitriding case, increased surface hardness, and greater case depth, as shown in Figure 4(b).

The hardness profile exhibits a peak hardness of approximately 1,246 HV at 525°C for 8 h, likely attributable to an optimal temperature and nitriding time balance, which promotes the formation of a high-hardness compound layer along with fine nitride precipitates. The surface hardness values attained reached 1,246 HV0.1, which represents approximately four times the hardness of the non-nitrided material (297 HV0.1). This significant enhancement in surface hardness can be ascribed to two principal factors: the generation of a high-hardness compound layer and the considerable lattice distortion induced by the diffusion of nitrogen atoms. When subjected to nitriding at 550°C, a maximum hardness of approximately 1,266 HV is attained after 6 h, potentially due to the supersaturation of nitrogen that induces increased distortion within the lattice, thereby optimizing the surface hardness. At 560°C, after an 8 h nitriding process, the hardness reaches a peak of around 1,141 HV, maintaining this value even after 12 h. At 570°C, the maximum hardness recorded is approximately 1,168 HV following 3 h of nitriding, subsequently decreasing to about 1,088 HV after 12 h. This diminished surface hardness at extended nitriding durations at elevated temperatures can be attributed to the formation of larger nitride precipitates. Over extended periods, the precipitate particles exhibit increased size and are more susceptible to coarsening, resulting in a lower density of precipitates and, consequently, reduced hardness. The initially observed high hardness is a direct consequence of the salt bath nitriding process, which promotes the rapid diffusion of nitrogen atoms into the steel surface, culminating in the formation of a hardened compound layer and a finely dispersed array of nitride precipitates. This diffusion phenomenon significantly augments surface hardness during the preliminary stages of nitriding, prior to the commencement of precipitate coarsening at prolonged durations.

From the findings, it is evident that once the nitriding temperature surpasses 550°C, specifically at 570°C, the microhardness of the specimen LN570°C after a duration of 12 h is measured at 1,088 HV0.1, which is comparatively lower than that of the other specimens. The observed decrease in hardness from the surface to the substrate indicates the existence of a diffusion zone, where the formation of precipitates comprising nitrides and additional metallic alloy nitrides occurs at both the grain boundaries and within the grains themselves. The LN550°C specimen after 6 h exhibits a notably increased microhardness profile within its surface layer in relation to the other specimens. The maximum thickness of the nitride layer, quantified at 92.00 µm, is documented for the sample subjected to nitriding at 570°C for 6 h. The surface hardness demonstrated an increase concomitant with the augmented duration and temperature of the salt bath nitriding treatment; however, prolonged nitriding intervals resulted in a marked decrease in the surface hardness at elevated temperatures due to the emergence of sizable nitride precipitates. The surface hardness is contingent upon the nitriding duration when the temperature remains constant; nevertheless, the corresponding case depths of the nitrided samples exhibit an increase with increasing temperatures.

3.3.2 Corrosion behavior

Electrochemical assessments are performed utilizing a 3.5 wt% NaCl electrolyte solution, employing a Biologic SP300 potentiostat managed by EC Lab software, operating at a scan rate of 0.5 mV/s to produce potentiodynamic anodic and cathodic polarization curves. Figure 6 illustrates the potentiodynamic polarization graphs of unmodified M50NiL steel in comparison to the LN specimens. The corrosion parameters, including Ecorr, Icorr, and the corrosion rate, are derived from the Tafel plots and are presented in Figure 5. In contrast to the untreated steel, the corrosion potential (Ecorr) of the nitrided specimens shifts toward a more noble potential, indicating a reduction in corrosion susceptibility. Both the untreated material and the nitrided specimens display cathodic passivation characteristics. Specifically, the untreated specimen records an Icorr of 108.2 μA, whereas the nitrided specimens manifest significantly lower values, as shown in Figure 5(a). This observation suggests that the nitrided samples exhibit superior corrosion resistance relative to their untreated counterparts.

The corrosion data illustrated in Figure 5(b) reveal that the LN525°C specimen at 08 h possesses an extended passive region, augmented polarization resistance, and diminished

corrosion current density, thereby indicating enhanced corrosion resistance. The presence of chromium nitrides (Cr4N and Cr2N), which are introduced during the LN process, likely facilitates the development of a passive chromium oxide layer atop the nitride layer, thereby further augmenting the overall corrosion resistance of the steel substrate. Given that nitrides are characterized as noble phases, a denser distribution of nitrides correlates with enhanced protective properties.

Upon nitriding at 525°C for 8 h, the specimen demonstrated a corrosion rate of 4.11 mpy, which is considerably lower than the untreated sample's rate of 49.57 mpy. Among the nitrided specimens, LN525 at 08 h exhibited the most favorable corrosion performance, with a corrosion current (Icorr) of 8.97 µA, which is substantially lower than that observed in the other samples. This improved corrosion performance can be partially ascribed to the specimen's significantly elevated microhardness, as a harder surface typically confers heightened resistance to both corrosion and wear. Additionally, lower sulfur content generally facilitates the formation of a thicker and more protective nitride layer, resulting in a decreased corrosion current density (Icorr). The LN525°C specimen at 08 h also demonstrated a more positive corrosion potential (Ecorr) of -442.9 mV in contrast to the untreated material, which exhibited -553.963 mV. Furthermore, the open-circuit voltage (OCV) measurement of -0.29 further corroborates that the nitrided steel LN525°C at 8 h possesses a less noble corrosion potential, emphasizing its superior corrosion resistance.

The LN550°C at 6 h specimen reveals a corrosion rate of 21.74 mpy, which is optimal for LN at 550°C, as shown in Figure 5(c). This exceptional corrosion resistance is attributable to the formation of a dense and uniform nitride layer that offers effective protection against corrosive environments while concurrently preserving the material's integrity by preventing the excessive brittleness that may arise from elevated nitrogen concentrations.

The LN560°C sample at 6 h displays a reduced passive range, as evidenced by Figure 5(d). This comparatively thin layer serves as a less effective protective barrier, resulting in a corrosion rate of 48.76 mpy, which parallels that of the untreated sample. Conversely, the LN560°C sample at 12 h exhibits markedly enhanced anodic kinetics, characterized by a corrosion current density (Icorr) of 157.68 µA. An increase in sulfur content typically facilitates the development of a fragile and less protective nitride layer, culminating in an elevated corrosion current density and a concomitant decrease in the material's corrosion resistance. Notably, the LN560°C sample at 12 h demonstrated the highest corrosion rate within the cohort, recorded at 72.2 mpy, indicating that LN under these conditions may be

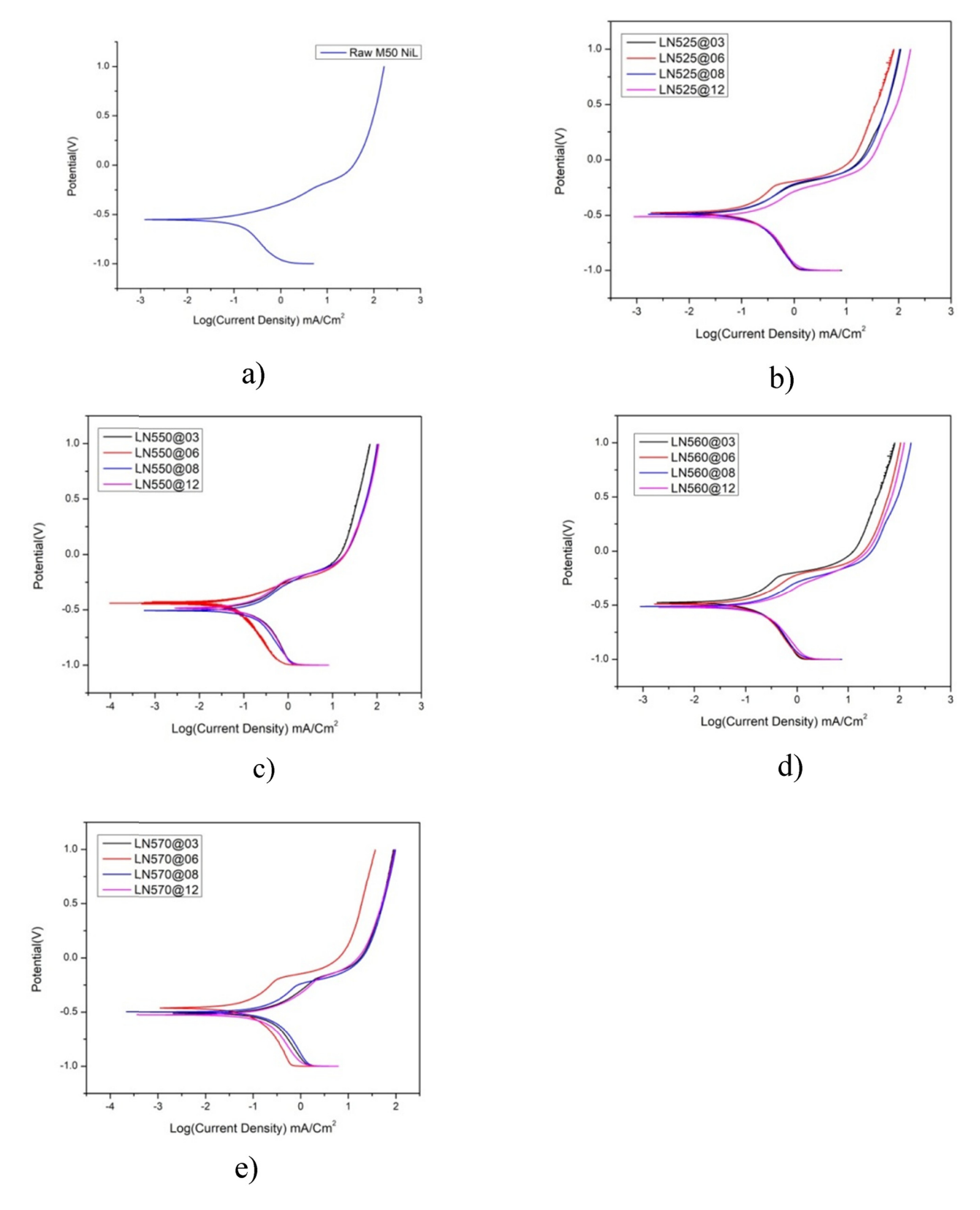


Figure 5: (a)–(e) Tafel plots of LN samples at 525, 550, 560 and 570°C for 3, 6, 8, and 12 h, respectively: (a) untreated sample, (b) Tp for LN525°C, (c) Tp for LN550°C, (d) Tp for LN560°C, and (e) Tp for LN570°C.

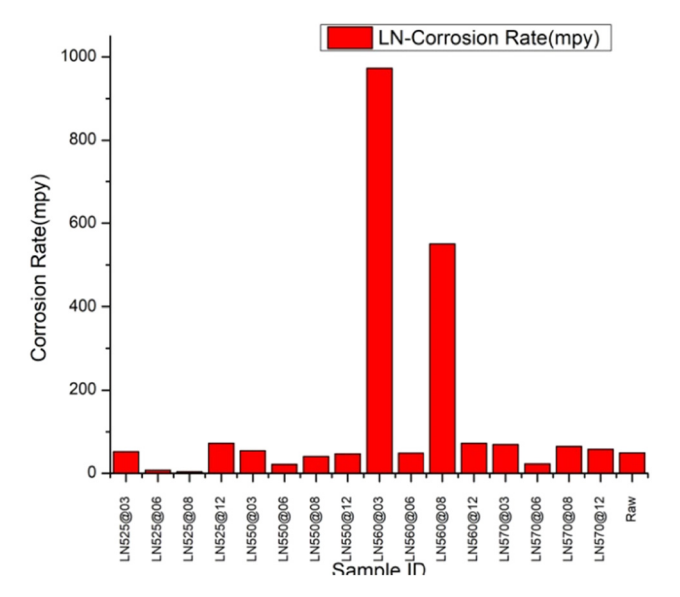


Figure 6: Corrosion rate for raw and LN samples.

ineffective, potentially attributable to augmented nitrogen diffusion resulting in material brittleness. Figure 5(e) illustrates an expansive passive range for the LN570°C sample at 6 h, presumably due to the formation of a more substantial nitride layer. This thicker layer functions as an efficient protective barrier, yielding a corrosion rate of 22.9 mpy, particularly under conditions of elevated temperature and limited duration.

The low-temperature LN samples exhibit extensive passive ranges, thereby substantiating that low-temperature LN not only enhances Ecorr but also significantly improves corrosion resistance, as shown in Figure 6. The 8 h LN process conducted at a lower temperature (525°C) on the LN525°C sample at 08 h appears to have markedly augmented its corrosion resistance. Following the nitriding temperature surpassing 550°C, particularly at 560°C, a substantially thick oxide layer envelops the sample's surface, with the presence of some cracks due to the considerable compressive stress. Previous findings have indicated that this oxide layer exhibits a markedly low hardness, thereby severely compromising corrosion resistance. However, nitriding for durations exceeding 12 h could precipitate material degradation and increased brittleness, thereby emphasizing the necessity of optimizing the nitriding duration.

Low-temperature LN exerts a significant impact on localized corrosion behavior. In contrast, all low-temperature LN samples reveal extensive passive ranges, indicating their high resistance to pitting corrosion. The current density remained stable and did not augment with potential when applied to a certain threshold for the treated samples. This observation suggests that passivation tendencies manifested

during anodic polarization. Conversely, anodic activation persisted in the untreated sample.

3.4 Tribological performance (Wear and COF)

A pin-on-disc tribometer represents the apparatus utilized for ascertaining the sliding friction coefficient and the wear volume of duplex-treated surfaces. Wear testing is conducted on both untreated and treated M50NiL specimens. The pin and ball disc friction and wear testing apparatus, TE-165-SPOD, produced by Magnum Engineers, is employed in the experimental investigation. The specimens are subjected to normal loading while sliding against a disc composed of EN24 steel. The pin-on-disc testing apparatus consists of a stationary pin subjected to an applied load, which remains in contact with a rotating disc. The resultant parameter, wear volume loss (WVL), is quantified utilizing a linear variable differential displacement transducer (LVDT) exhibiting an accuracy of ±1 and further determined with the assistance of a load cell exhibiting a range of 0-200 N. The tests are executed in accordance with the ASTM G99-04 standard. Figure 7(a)-(e) illustrates the friction coefficients and wear rates of the untreated and nitrided M50NiL steel specimens, which are tested against a WC ball for a duration of 3,600 s under a load of 20 N. The nitrided specimens demonstrate relatively consistent friction coefficients attributable to the elevated hardness of the nitrides present on the modified surface. The friction coefficient of the untreated specimen is recorded as 0.5773, which exceeds those of the nitrided specimens. This observation indicates that the development of a nitrided layer not only augments surface hardness but also enhances friction characteristics.

From Figure 7(a), it is observable that the LN550°C specimen at 3 h manifests a friction coefficient of 0.27865, which is inferior to that of the other specimens. In comparison to the untreated specimen, the friction coefficients of the nitrided specimens are reduced during the initial phase, subsequently rising to a stable condition. In the stable phase, the friction coefficients of the nitrided samples at 525°C for 8 h, 550°C for 12 h, 560°C for 8 h, and 570°C for 6 h are approximately 0.2782, 0.3425, 0.3372, and 0.3272, respectively. The friction coefficient of the nitrided specimens exhibits an increase relative to both treatment duration and temperature. The LN560°C specimen at 3 h displays elevated friction coefficients when subjected to a load of 20 N. To further elucidate the wear characteristics of the untreated and plasma-nitrided specimens, the volume wear rates of the specimens are presented in Figure 7(e).

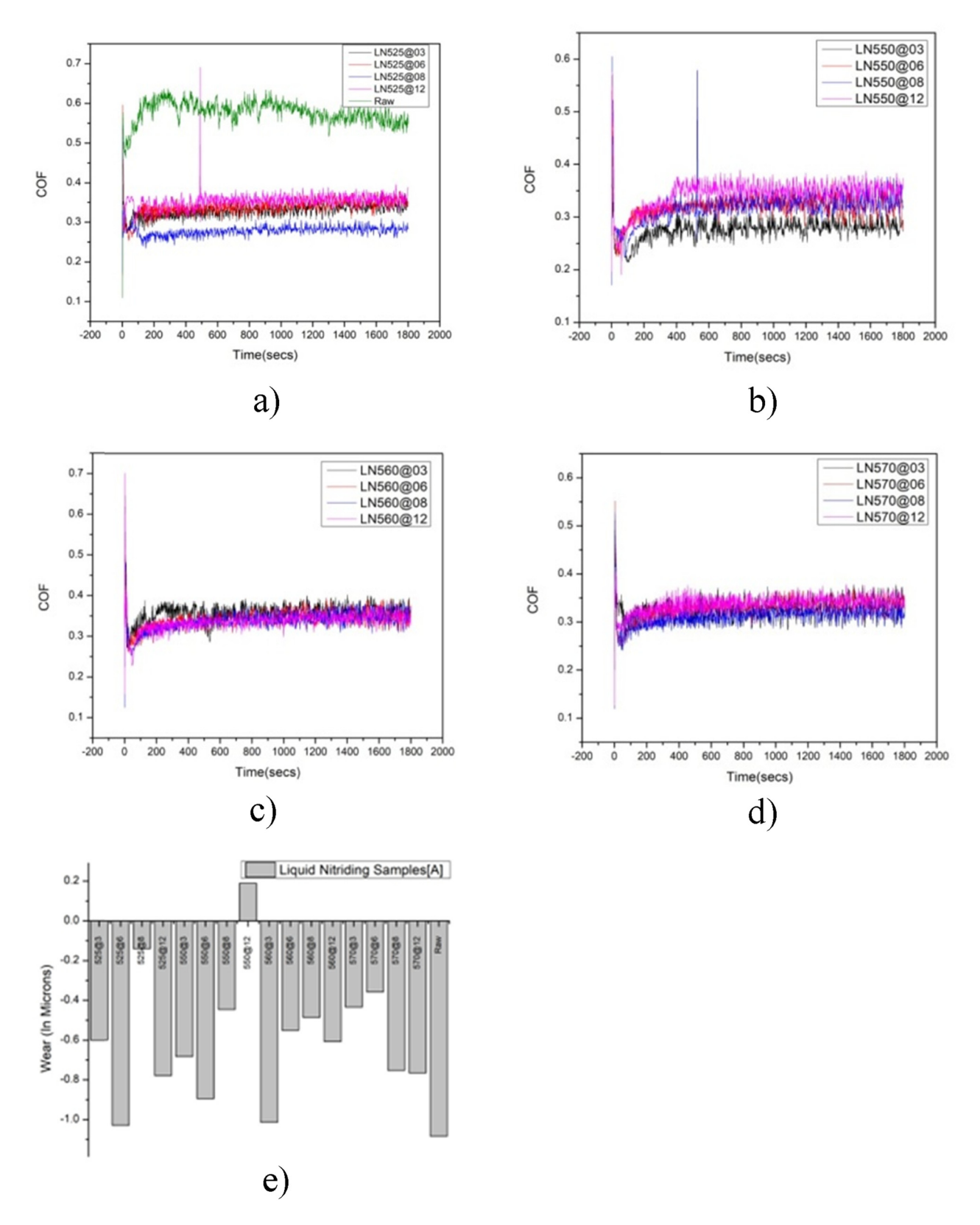


Figure 7: (a)–(e) COF of the specimens treated at 3, 6, 8, and 12 h for different nitriding temperatures: (a) COF for LN525°C, (b) COF for LN550°C, (c) COF for 560°C, (d) COF for LN570°C, and (e) WR of untreated and nitrided LN Samples.

As shown in Figure 7(a), the LN525°C specimen at 8 h exhibits an exceptionally low wear rate of 0.02×10^{-6} g/m (-0.13935) alongside a friction coefficient of 0.2782, which is remarkably low for a sample subjected to nitriding at 525°C. Furthermore, this specimen displays the highest levels of hardness and corrosion resistance among the evaluated samples, rendering it particularly effective in enhancing both wear and corrosion characteristics. In juxtaposition, the untreated specimen presents a substantially elevated wear rate of 0.52×10^{-6} g/m (-1.08422). Among the specimens that are nitrided at 525°C, the one demonstrating the most significant wear resistance is the LN525°C sample at 8 h, as evidenced by its minimal wear rate. The surface microstructures of the LN525°C specimen at 8 h indicate that the \(\epsilon - \text{Fe}_{2-3} \text{N} \) phase, which formed during the LN process at 525°C, is advantageous in augmenting wear resistance. This particular phase, characterized by its structural attributes, possesses elevated atomic binding energies, thereby contributing to enhanced wear resistance. Consequently, the LN525°C at 8 h sample possesses the lowest wear rate among the specimens subjected to testing. The LN525°C specimen at 6 h displays an increased rate of 0.52×10^{-6} g/m (-1.02969), which is comparable to that of the untreated sample. This elevated wear rate may be ascribed to an inadequate duration of nitriding, which likely culminated in a thinner and less protective nitride layer. The specimen also presents a friction coefficient of 0.3387, indicating reduced wear resistance in comparison to the other nitrided samples.

The LN550°C specimen at 12 h has exhibited a low wear rate of 0.05×10^{-6} g/m (0.18932), which is inferior to that of other samples subjected to treatment at 560°C, as shown in Figure 7(b). The wear resistance is notably most pronounced in the LN550°C specimen at 12 h, likely attributable to the development of an approximately 82 µm thick, robust nitride layer formed during the 12-h LN procedure. This durable layer substantially enhances the wear resistance of the specimen. The wear resistance of the LN550°C specimen at 12 h is significantly greater than that of all other nitrided samples, with a value of 25000000.000 \times 10⁻³ N m/mm³. This superior wear resistance can be ascribed to the optimized thickness and composition of the nitride layer achieved following the 12-h treatment duration. This phenomenon may be elucidated by the presence of a thick layer composed of hard nitrides resulting from the prolonged LN process.

The LN560°C sample subjected to an 8 h treatment has demonstrated a notably low wear rate of 0.25×10^{-6} g/m (-0.48487), indicating exceptional wear resistance in comparison to other specimens subjected to nitriding at 560°C, as shown in Figure 7(c). This remarkable wear resistance can be attributed to the optimal interplay between the thickness of the nitride layer and the hardness attained during the 8h nitriding process, which proficiently safeguards the surface against wear while preserving the structural integrity of the material.

The LN570°C sample treated for 6 h has exhibited a lower wear rate of 0.16×10^{-6} g/m (-0.35637) in relation to other samples nitrided at 570°C, as shown in Figure 7(d). This improvement in wear resistance is presumably a consequence of the meticulous regulation of nitrogen diffusion at 570°C, culminating in a precisely engineered nitride layer that offers substantial surface protection without undermining the toughness of the material.

The wear rates of the untreated material alongside samples nitrided at various temperatures are illustrated in Figure 7(e), revealing a reduction in wear rate concomitant with an increase in processing temperature. The wear volume for the LN specimens treated at 525°C for 8 h, 550°C for 12 h, 560°C for 8 h, and 570°C for 6 h, under an applied load of 20 N and a sliding speed of 1,909 rpm, are determined to be 0.017×10^{-3} mm³/m, 0.031×10^{-3} mm³/m, 0.094 \times 10⁻³ mm³/m, and 0.063 \times 10⁻³ mm³/m, respectively, for a sliding distance of 3,600 m.

4 Conclusion

M50 NiL steel specimens with different temperatures ranging from 525 to 570°C with durations of 3, 6, 8, and 12 h are investigated to identify the phase structure, microstructural changes, wear, corrosion, and micro-hardness, and the major outcomes are as follows:

- (a) The LN layer comprises a diffusion layer, and subsequent to the nitriding process, phases such as α-FeN, y-FeN, and y-Fe₃N, along with Fe₃O₄, are generated on the surface layer of M50 NiL. Moreover, substantial concentrations of nitrogen are observed in the LN at a temperature of 560°C for 12 h.
- (b) The microhardness of M50 NiL LN specimens subjected to a temperature of 550°C for 6 h is recorded at 1266 HV, which is fivefold greater than that of the untreated specimen, which measures 294 HV, a difference that may be attributed to the significant presence of large primary carbides during the assessment.
- (c) The wear resistance and friction coefficient of M50 NiL LN specimens treated at 500°C for 12 h indicate a minimal wear rate of $0.05 \times 10^{-6} \, \text{g/m} \, (0.18932 \, \mu\text{m})$ alongside a friction coefficient of 0.3425, in contrast to the untreated sample, which exhibits a wear rate of 0.52×10^{-6} g/m (-1.08422 µm) and a friction coefficient of 0.5773. It is evident that the friction coefficient

- and wear rate of the nitrided specimens are markedly lower than those of the untreated samples.
- (d) The corrosion resistance behavior of the M50 NiL nitride sample is significantly improved for 525°C at 8 h, the specimen showed a corrosion rate of 4.110 mpy, significantly lower than the untreated sample's rate of 49.577 mpy. In the future, to identify the significant growth in surface properties, optimization processes like genetic algorithms can be used to minimize the experiments, and also approach like fuzzy logic can predict the surface hardness based on case depth data given as input to the monitoring system.

Funding information: This work was funded by the Aeronautical Research and Development Board, New Delhi, under research grants (1957). The authors acknowledge the support of ARDB for this article.

Author contributions: Venkatesh and Kasi V Rao designed the experiments, and Anil carried them out. Nageshwara Rao developed the model for characterization. Anil prepared the manuscript with guidance from all co-authors. All authors have accepted responsibility for the entire content of this manuscript and approved its submission.

Conflict of interest: Authors state no conflict of interest.

Data availability statement: Data sharing is not applicable to this article as no datasets were generated or analyzed during the current study.

References

[1] Yan J, Wang J, Gu T, Pan D, Wang DQ, Lin YH, et al. Effect of liquid nitriding at 400–670°C on microstructure and properties of C110 steel. J Cent South Univ. 2017;24(2):325–34.

- Balikci E, Yaman O. Investigation on liquid bath nitriding of selected steels. Surf Eng. 2011;27(8):609–15.
- [3] Venkata Suresh J, Manivardhan Reddy K, Reddy BGK, Naga Malleswara Rao DS, Keerthi Reddy G, Aparna S, et al. Assessment of wear behavior on treated AISI 310 by liquid nitriding process. AIP Conf Proc. 2024;3007:100037.
- [4] Ravi Shankar R, Saravanan R, Senthil J. Experimental investigation of metallurgical behaviors of liquid, gas & plasma nitrided steel. Proc Natl Conf Recent Trends Mech Eng. 2014;1(14):88–98.
- [5] Li L, Wang J, Yan J, Duan L, Li X, Dong H. The effect of liquid nitriding on the corrosion resistance of AISI 304 austenitic stainless steel in H₂S environments. Metall Mater Trans A. 2018;49:6521–32.
- [6] Michla JRJ, Ravikumar B, Ram Prabhu T, Siengchin S, Arul Kumar M, Rajini N. Effect of nitriding on mechanical and microstructural properties of direct metal laser sintered 17-4PH stainless steel. J Mater Res Technol. 2022;19(7):2810–21.
- [7] Fu H, Zhang J, Huang J, Lian Y, Zhang C. Effect of temperature on microstructure, corrosion resistance, and toughness of salt bath nitrided tool steel. J Mater Eng Perform. 2016;25(1):3–8.
- [8] Kumar N, Chaudhari GP, Meka SR. Investigation of lowtemperature liquid nitriding conditions for 316 stainless steel for improved mechanical and corrosion response. Trans Indian Inst Met. 2020;73(1):235–42.
- [9] Monteiro WA, Pereira SA, Vatavuk J. Nitriding process characterization of cold worked AISI 304 and 316 austenitic stainless steels. J Metall. 2017;1:1–7.
- [10] Zhang X, Wang J, Fan H, Pan D. Erosion-corrosion resistance properties of 316L austenitic stainless steels after low-temperature liquid nitriding. Appl Surf Sci. 2018;440(SI2):755–62.
- [11] Somers MAJ, Christiansen TL. Nitriding of steels. Encycl Mater: Met Alloy. 2022;2(2):173–89.
- [12] Reddy CAK, Srinivasan T, Venkatesh B. Effect of plasma nitriding on M50 NiL steel – A review. Mater Today Proc. 2022;52(3):1073–7.
- [13] Venkatesh B, Reddy CAK. Investigation on nitriding and microstructure evolution of M50 NiL steel: A review. Innov Mech Eng. Lect Notes Mech Eng. 2022;I(21):579–89. Springer.
- [14] Venkatesh B, Reddy CAK. Experimental study on heat treatment and mechanical behaviour of M50 NiL steel – A review. Mater Today Proc. 2021;46(1):795–8.
- [15] Korotkov VA, Isakov DV. Influence of liquid nitriding on the properties of the electric steel 10. IOP Conf Ser: Mater Sci Eng. 2020;966(1):012006.
- [16] Ghelloudj E, Djebaili H, Hannachi MT, Saoudi A, Daheche B. The influence of salt bath nitriding variables on hardness layer of AISI 1045 steel. Acta Metall Slov. 2016;22(3):188–94.